

# Charge-State Distributions after Beta Decay of ${}^6\text{He}$ to Form ${}^6\text{Li}^+$

Aaron T. Bondy <sup>1,\*</sup>  and Gordon W. F. Drake <sup>1,2</sup> <sup>1</sup> Department of Physics, University of Windsor, Windsor, ON N9B 3P4, Canada<sup>2</sup> Canterbury College, Windsor, ON N9B 3Y1, Canada

\* Correspondence: bondy11u@uwindsor.ca

**Abstract:** The shake-off processes and charge-state fractions of  ${}^6\text{Li}^+$ ,  ${}^6\text{Li}^{++}$ , and  ${}^6\text{Li}^{3+}$  were studied following the beta decay of  ${}^6\text{He}$  in the  $1s^2\ 1S_0$ ,  $1s2s\ 1S_0$ , and  $1s2s\ 3S_1$  initial states. The sudden approximation was used, together with fully correlated Hylleraas wave functions and pseudostates. A projection operator method was introduced to separate the charge-state fractions in the positive energy region of overlapping continua. The results show that  ${}^6\text{Li}^{++}$  (single-ionisation) remains dominant, even in the energy range  $E > 0$ , where the formation of  ${}^6\text{Li}^{3+}$  (double-ionisation) is energetically allowed. The results reduce disagreements with the experiment for the fraction of  ${}^6\text{Li}^{3+}$  by nearly an order of magnitude, but substantial disagreements remain that are inconsistent with the sudden approximation widely used in other similar work.

**Keywords:** beta decay; double-ionisation; two-electron calculations; Hylleraas wave functions; Sturmian projectors

## 1. Introduction

There has been a long-standing interest in the beta decay of the halo nucleus  ${}^6\text{He}$  to form  ${}^6\text{Li}^+$  according to the Gamow–Teller process [1–3]:



especially in connection with searches for new physics beyond the Standard Model [4–7]. In this context, all single beta decay processes are thought to be either of the Fermi  $V$ -type, where the beta particle ( $e^-$ ) and the antineutrino ( $\bar{\nu}$ ) are coupled to form a total spin of 0 or the Gamow–Teller  $A$ -type, where  $e^-$  and  $\bar{\nu}$  are coupled to form a total spin of 1. The  ${}^6\text{He}$  decay process is thought to be an example of the latter. In the former case, the angular correlation coefficient between the  $e^-$  and the  $\bar{\nu}$  is 1, and in the latter case, it is  $-1/3$  [8]. Any deviation from these angular correlations could therefore be interpreted as a signal for new physics.

The classic experiment by Carlson et al. [1] measured the angular correlation coefficient in  ${}^6\text{He}$  decay with helium atoms prepared in the ground  $1s^2\ 1S_0$  state. In addition, there has been an ongoing experiment [9] involving metastable  $1s2s\ 3S_1$  helium atoms held in an MOT trap. Müller et al. recently demonstrated [10] the first precise determination of the angular correlation coefficient using  ${}^6\text{He}$  decay with a neutral trap and found results consistent with the Standard Model. The challenge in both experiments is that the  $\bar{\nu}$  cannot be detected directly, and so, its momentum vector must be deduced from the overall kinematics of the decay process, including both the  $\beta$  particle and the recoiling  ${}^6\text{Li}$  nucleus, together with its two atomic electrons. Any additional momentum carried away by the atomic electrons must, therefore, be included in the kinematics if one or both of them are emitted in subsequent ionisation events (shake-off). Otherwise, deviations due to the electronic momentum might masquerade as a signal for new physics.

With shake-off processes included, the possible final states are, thus,  ${}^6\text{Li}^+$ ,  ${}^6\text{Li}^{++}$ , and  ${}^6\text{Li}^{3+}$ . Although there is reasonably good agreement between the theory and experiments



**Citation:** Bondy, A.T.; Drake, G.W.F. Charge-State Distributions after Beta Decay of  ${}^6\text{He}$  to Form  ${}^6\text{Li}^+$ . *Atoms* **2023**, *11*, 41. <https://doi.org/10.3390/atoms11030041>

Academic Editors: Ulrich D. Jentschura and Alexander Kramida

Received: 27 January 2023

Revised: 18 February 2023

Accepted: 19 February 2023

Published: 23 February 2023



**Copyright:** © 2023 by the authors. Licensee MDPI, Basel, Switzerland. This article is an open access article distributed under the terms and conditions of the Creative Commons Attribution (CC BY) license (<https://creativecommons.org/licenses/by/4.0/>).

for the  ${}^6\text{Li}^+$  and  ${}^6\text{Li}^{++}$  charge-state fractions, as shown in Table 1, there is a large disagreement for the small amount of  ${}^6\text{Li}^{3+}$  corresponding to double-ionisation, with the theory predicting one or two orders of magnitude more than what is observed in experiments. The disagreement is equally evident for both  ${}^6\text{He}(1s^2\ 1S_0)$  [1] and  ${}^6\text{He}(1s2s\ 3S_1)$  [9] as the initial states. The table shows comparisons with both our own previous calculations based on fully correlated Hylleraas wave functions [11] and with earlier configuration interaction (CI) calculations by Wauters and Vaeck [2]. In contrast, there is excellent agreement between the theory and experiments for the charge-state fractions of  ${}^6\text{Li}^{++}$  and  ${}^6\text{Li}^{3+}$  following beta decay in the one-electron case of  ${}^6\text{He}^+(1s_{1/2})$  [3], indicating that the sudden approximation (see Section 2) universally used in past work is evidently well justified.

This paper is organised as follows. In Section 2, we present a formulation of the problem within the sudden approximation and, in Section 3, we develop a projection operator method based on products of hydrogenic wave functions to separate the charge-state fractions in the energy region of overlapping continua for  ${}^6\text{Li}^{++}$  and  ${}^6\text{Li}^{3+}$ . Perturbative corrections to the projection operators due to the electron–electron interaction are calculated and shown to be small. The results in Section 4 show that, while the projection operators substantially reduce the disagreement with the experiment, the predicted amount of  ${}^6\text{Li}^{3+}$  is still larger by an order of magnitude. Possible further corrections and other applications of the projection operator method are discussed in the final Discussion Section 4. The abbreviated notations  $1\ 1S_0$ ,  $2\ 3S_1$ , and  $2\ 1S_0$  are used for the ground low-lying metastable states  $1s^2\ 1S_0$ ,  $1s2s\ 3S_1$ , and  $1s2s\ 1S_0$ , respectively.

**Table 1.** Comparison of the previous theory with experiments for the probabilities  $p({}^6\text{Li}^{k+})$  of forming the various charge states with  $k = 1, 2, 3$  following the beta decay of  ${}^6\text{He}(1\ 1S_0)$  or  ${}^6\text{He}(2\ 3S_1)$  as the initial states. All quantities are expressed in percent (%).

${}^6\text{He}$ State	Li-Ion	Theory [11]	Theory [2]	Exp't.
$1\ 1S_0$	${}^6\text{Li}^+$	89.03(3)	89.09	89.9(2) <sup>a</sup>
	${}^6\text{Li}^{++}$	9.7(1)	10.44	10.1(2)
	${}^6\text{Li}^{3+}$	1.2(1)	0.32	0.018(15)
	Total	99.9(1)	99.85	100.0(2)
$2\ 3S_1$	${}^6\text{Li}^+$	88.711(3)		89.9(3)(1) <sup>b</sup>
	${}^6\text{Li}^{++}$	9.42(7)		10.1(3)(1)
	${}^6\text{Li}^{3+}$	1.86(7)		<0.01
	Total	99.99(7)		100.00

<sup>a</sup> Carlson et al. [1]. <sup>b</sup> Hong et al. [9].

## 2. Formulation of the Problem

The kinematics of the process is as follows. As discussed previously [9,11], the emitted  $\beta$  particle has a maximum kinetic energy of  $E_{\text{max}} = 3.51$  MeV with a broad energy distribution going down to nearly zero. However, in the experiment of Hong et al. [9], only those events with  $E > 1$  MeV were counted. At these energies, the  $\beta$  particle is relativistic. From the relativistic energy–momentum equation  $(E_{\text{max}} + m_e c^2)^2 = c^2 p^2 + m_e^2 c^4$ , the maximum recoil momentum is  $P_{\text{rec}} = 1070$  a.u. In contrast, since the recoiling  ${}^6\text{He}$  nucleus is much more massive ( $M = 6.01523$  u), its recoil velocity of  $v_{\text{rec}} = 0.0925$  a.u. is nonrelativistic. In addition, the corresponding recoil momentum  $\hbar K = m_e v_{\text{rec}}$  transferred to the atomic electrons is so small that it is unimportant for the purposes of the present discussion. In particular, the probability for the formation of  $\text{Li}^{3+}$  can be written in the form [11]:

$$P(\text{Li}^{3+}) = A + K^2 B + \dots \tag{2}$$

with  $B \simeq 0.005$  so that  $K^2 B \simeq 4 \times 10^{-5}$  relative to the previously calculated value  $A \simeq 0.012$ . The present work, therefore, focused on the leading  $A$  term and neglected the recoil.

Additional exchange effects between the  $\beta$  particle and the atomic electrons have also been considered and found to be negligible at these energies [12,13].

With these approximations, the emitted  $\beta$  particle can be thought of as a spherical shell of charge expanding with (nearly) the velocity of light. Past work [1–3,11] has always made use of the sudden approximation in which the Coulomb pulse is taken to be instantaneous and the initial helium wave function  $\Psi(^6\text{He})$  is expanded over the complete set of states  $\Psi_i(^6\text{Li}^+)$  according to

$$e^{i\mathbf{K}\cdot(\mathbf{r}_1+\mathbf{r}_2)}\Psi(\text{He}) = \sum_i c_i\Psi_i(\text{Li}^+) \tag{3}$$

where  $\hbar\mathbf{K}$  is the recoil momentum of the  $^6\text{Li}^+$ -ion and the sum over  $i$  includes an integration over both the single- and double-electron ionisation continua to form  $^6\text{Li}^{++}$  and  $^6\text{Li}^{3+}$ , respectively. The factor  $e^{i\mathbf{K}\cdot(\mathbf{r}_1+\mathbf{r}_2)}$  generates the transformation to the moving frame of reference. Recoil corrections are important for the analysis of experiments [11], but for the present study, we worked in the limit of zero recoil ( $\mathbf{K} = 0$ ) since the recoil effects do not materially change the charge-state distributions, which are our main focus. The absolute squares:

$$|c_i|^2 = |\langle\Psi_i(\text{Li}^+) | \Psi(\text{He})\rangle|^2 \tag{4}$$

are then the transition probabilities into the various final states. Although there is reasonably good agreement between the theory and experiments for the  $^6\text{Li}^+$  and  $^6\text{Li}^{++}$  charge-state fractions, there is a large disagreement for the small amount of  $^6\text{Li}^{3+}$  corresponding to double-ionisation. The analysis is compounded by the fact that the  $^6\text{Li}^{++}$  continuum underlies the  $^6\text{Li}^{3+}$  continuum for positive energies above the  $E = 0$  threshold for the formation of  $^6\text{Li}^{3+}$  (see Figure 1). The two charge states must, therefore, be separated in the calculations involving the positive energy range.

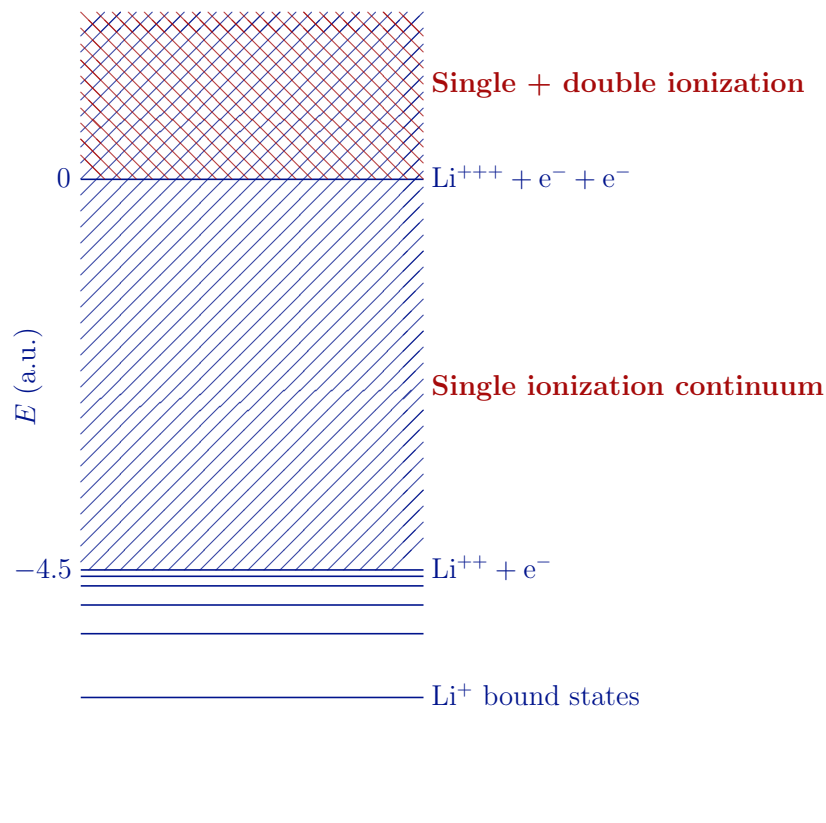


**Figure 1.** Energy level diagram for  $^6\text{Li}^+$  following the beta decay. For the  $E > 0$  region, the single-ionisation continuum underlies the double-ionisation continuum, and so, both charge states contribute to the total.

Our previous calculations of the charge-state distribution [11] in fact partitioned the possible final states by their energy range (bins), as in Figure 1, rather than the charge state, according to

$$\begin{aligned}
 \text{Bin 1 :} & \quad E_g(\text{Li}^+) \leq E < E_g(\text{Li}^{++}) \\
 \text{Bin 2 :} & \quad E_g(\text{Li}^{++}) \leq E < E_g(\text{Li}^{3+}) \\
 \text{Bin 3 :} & \quad E_g(\text{Li}^{3+}) \leq E < \infty
 \end{aligned} \tag{5}$$

where  $E_g(\text{Li}^+) = -7.2799134 \dots$  a.u. is the ground-state energy of  ${}^6\text{Li}^+$ ,  $E_g(\text{Li}^{++}) = -4.5$  a.u., and  $E_g(\text{Li}^{3+}) = 0$ . Bins 1 and 2 by definition consist entirely of  ${}^6\text{Li}^+$  and  ${}^6\text{Li}^{++}$ , respectively, but Bin 3 contains contributions from both  ${}^6\text{Li}^{++}$  and  ${}^6\text{Li}^{3+}$ . The principal aim of the present work was to resolve Bin 3 into its charge-state components.

One can see from phase-space arguments that the fraction of  ${}^6\text{Li}^{3+}$  is strongly suppressed near the threshold because the energy above the  $E = 0$  threshold must be equally shared between the two outgoing electrons. Otherwise, one electron will fall back to a bound state of  ${}^6\text{Li}^{++}$ , and the other will escape with all the excess energy. It is, therefore, necessary to project out of the various pseudostates  $\Psi_i$  satisfying  $E_i > 0$  the  ${}^6\text{Li}^{3+}$  component.

The problem of calculating the final-state fraction of  ${}^6\text{Li}^{3+}$  to  ${}^6\text{Li}^{++}$  is closely related to the problem of calculating the ratio of photoionisation cross sections  $R = \sigma(\text{Li}^{3+})/\sigma(\text{Li}^{++})$ , on which there is a vast and rich literature for helium, ranging from many-body perturbation theory (MBPT) [14–16], close-coupling (cc) [17], convergent close-coupling (ccc) [18], R-matrix methods [19] with a discretisation of the continuum, and various distorted wave (DW) approximations for the final-state wave function [20–23]. The older literature up to 1996 was reviewed by Sadeghpour [24]. More recent work has applied these same methods to single- and double-photoionisation of  ${}^6\text{Li}^+$ , including R-matrix calculations [25,26], time-dependent close-coupling (TDCC) [27], ccc for the helium isoelectronic sequence [28], and B-spline methods [26,29]. The use of the method presented in this paper for the problem of double-photoionisation in helium is currently at a preliminary stage of investigation. This method is complementary to those mentioned above in that it uses the behaviour of the wave function as  $r \rightarrow 0$  as opposed to the more common asymptotic condition as  $r \rightarrow \infty$ .

The present work starts with discrete variational representations of the initial and final states in terms of fully correlated wave functions in Hylleraas coordinates of the form [30,31]:

$$\Psi = \sum_{ijk}^{i+j+k \leq \Omega_2} \left[ \underbrace{c_{ijk}^{(A)} \varphi_{ijk}(\alpha_A, \beta_A)}_{\text{A-sector}} + \underbrace{c_{ijk}^{(B)} \varphi_{ijk}(\alpha_B, \beta_B)}_{\text{B-sector}} \right] \tag{6}$$

where the basis functions  $\varphi_{ijk}(\alpha, \beta)$  are defined by

$$\varphi_{ijk}(\alpha, \beta) = r_1^i r_2^j r_{12}^k e^{-\alpha r_1 - \beta r_2} \mathcal{Y}_{l_1, l_2, L}^M(\hat{r}_1, \hat{r}_2) \pm \text{exchange}$$

The quantity  $\mathcal{Y}_{l_1, l_2, L}^M(\hat{r}_1, \hat{r}_2)$  represents a vector-coupled product of spherical harmonics of angular momenta  $l_1$  and  $l_2$  to form a state with total angular momentum  $L$  and component  $M$ . The parameter  $\Omega_2 = (i + j + k)_{\text{max}}$  controls the size  $N_2$  of the basis set. The basis set is “doubled” in the sense that the same combination of powers  $(i, j, k)$  occurs twice for different nonlinear parameters  $\alpha_A, \beta_A$  and  $\alpha_B, \beta_B$ , which characterise the asymptotic (A) and short-range (B) sectors, respectively. Diagonalisation of the Hamiltonian matrix in an orthogonalised basis set then determines a set of  $N_2$  eigenvectors that form a pseudospectral presentation of the actual spectrum of bound and continuum states. The nonlinear parameters are determined by calculating analytically the four derivatives  $\partial E/\partial \alpha_X$  and  $\partial E/\partial \beta_X$  and finding the zeros by Newton’s method for a particular state of interest. For the pseudostates, the parameter  $\beta_A$  was adjusted to give a variational extremum for the

${}^6\text{Li}^+$  charge-state fraction. The pseudostates represent a two-electron generalisation of a Coulomb Sturmian basis set for hydrogen.

The basic premise of the present work was that these fully correlated pseudostates  $\Psi_i({}^6\text{Li}^+)$  on the right-hand-side of Equation (3) contain complete information about all possible two-electron states, including single- and double-continuum states, as well as autoionising resonances, at least in the limit of large basis sets and in the region of space near the nucleus. The reason for believing this to be true is that the same basis sets accurately satisfy a range of oscillator strength sum rules such as the Thomas–Reiche–Kuhn (TRK) sum rule [32,33]:

$$\sum_i f_{0,i} = N \tag{7}$$

where  $N = 2$  for a two-electron atom, and other similar types of closure relations. Several such sum rules were tested and found to be accurately satisfied in our previous work [11], including a generalised TRK sum rule that includes the change in Coulomb potential accompanying beta decay. The use of a discrete variational representation in [11] supplemented by Stieltjes imaging techniques (a methodology on which this work directly built) allowed for accurate calculations by Goldman and Drake of the photoionisation cross section in hydrogen [34]. In fact, the same principle is contained in the assumption underlying Equation (3) that a helium wave function  $\Psi({}^6\text{He})$  can be expanded in terms of a complete set of pseudostates  $\Psi_i({}^6\text{Li}^+)$  constructed from fully correlated Hylleraas-type wave functions. The sum rules interconnect and tightly constrain the calculated charge-state fractions.

The central problem then is to construct a projection operator  $P$  and its orthogonal complement  $Q$  such that  $P | \Psi_i({}^6\text{Li}^+) \rangle$  corresponds to states where both electrons have asymptotically outgoing boundary conditions and such that  $P | \Psi_i({}^6\text{Li}^+) \rangle = 0$  for states lying below the double-ionisation threshold. Our strategy was to resolve each pseudostate  $| \Psi_i({}^6\text{Li}^+) \rangle$  lying above the double-ionisation threshold at  $E = 0$  into its orthogonal component parts  $|c_i^{3+}|^2 = \langle \Psi_i({}^6\text{Li}^+) | P | \Psi_i({}^6\text{Li}^+) \rangle$  and  $|c_i^{++}|^2 = \langle \Psi_i({}^6\text{Li}^+) | Q | \Psi_i({}^6\text{Li}^+) \rangle$ , where

$$R_i^{3+} = |c_i^{3+}|^2 / |c_i|^2 \tag{8}$$

$$R_i^{++} = |c_i^{++}|^2 / |c_i|^2 \tag{9}$$

are the fractional probabilities for the formation of  ${}^6\text{Li}^{3+}$  and  ${}^6\text{Li}^{++}$ , respectively. As usual, the projection operators have the properties  $P + Q = 1$  and  $PQ = 0$ .

### 3. Construction of Projection Operators

Our approach was to construct projection operators for the correlated two-electron pseudostates  $\Psi_i(\mathbf{r}_1, \mathbf{r}_2)$  in terms of the sums of the products of one-electron pseudostates  $\phi_n(\mathbf{r})$ . They were obtained by first orthogonalising and then diagonalising the unscreened hydrogenic Hamiltonian:

$$H_0 = -\frac{1}{2}\nabla^2 - Z/r \tag{10}$$

in a basis set of functions  $\chi_{j,k}(\mathbf{r}) = r^j e^{-\alpha\lambda^k r}$  for a range of powers  $j$  and  $k$  such that a particular  $\phi_{nl}(\mathbf{r})$  for angular momentum  $l$  has the form (for example):

$$\begin{aligned} \phi_{nl}(\mathbf{r}) = & [(a_{10} + a_{11}r + a_{12}r^2 + a_{13}r^3)e^{-\alpha\lambda r} \\ & + (a_{20} + a_{21}r + a_{22}r^2)e^{-\alpha\lambda^2 r} \\ & + (a_{30} + a_{31}r)e^{-\alpha\lambda^3 r} \\ & + (a_{40})e^{-\alpha\lambda^4 r}] r^l Y_l^m(\theta, \phi) \end{aligned} \tag{11}$$

for the case  $\Omega_1 = 4$ , where  $\Omega_1 = (j + k)_{\max}$ , and  $a_{st}$  are linear variational parameters. Because of their shape, we call these “triangular” basis sets, as used previously in the calculation of the Bethe logarithms for hydrogen [35]. The total number of terms is

$N_1 = \Omega_1(\Omega_1 + 1)/2$  if all terms in Equation (11) are kept. The triangular basis sets have two important features. First, the highest eigenvalue is pushed up by many orders of magnitude beyond what is typically achieved with a single exponential term (i.e., a “linear” basis set). For our typical values of  $\alpha = 0.1Z$  and  $\lambda = 5.15$ , the highest eigenvalue is approximately  $E_{\text{high}} = 10^{0.715\Omega_1 - 3.61}$  a.u., or  $2.5 \times 10^6$  a.u. The basis set, therefore, spans a huge range of (nonrelativistic) energy and distance scales. The ground state and first several excited states are also well represented. Second, the basis set has a remarkable degree of numerical stability, despite the huge range of distance scales covered. With quadruple precision,  $\Omega$  can be increased to around 17 or 18. As shown previously [35], the positive eigenvalues are roughly evenly spaced on a logarithmic energy scale up to very high energies. Quadruple precision was used throughout the calculations.

Assume for simplicity that  $\Psi_i(\mathbf{r}_1, \mathbf{r}_2)$  is an S-state. Neglecting the  $1/r_{12}$  electron–electron interaction, a zero-order approximation to the  $P$  projection operator can then be formed from a doubly positive energy sum over all (anti)symmetrised products of one-electron pseudostates:

$$P^{(0)} = \sum_l \sum_{n_+} |n_+, l\rangle \langle n_+, l| \tag{12}$$

where the sum over  $l$  is a sum over two-electron partial waves coupled to form an S-state and  $n_+$  stands for a pair of integers  $\{n, n'\}$  such that both  $\phi_{n,l}(\mathbf{r})$  and  $\phi_{n',l}(\mathbf{r})$  lie in the positive energy scattering continuum.  $|n_+, l\rangle$  is then correspondingly defined by

$$|n_+, l\rangle = \frac{1}{\sqrt{2}} [ | \phi_{n,l}(\mathbf{r}_1) \rangle | \phi_{n',l}(\mathbf{r}_2) \rangle \mathcal{Y}_{l0}^0(\hat{\mathbf{r}}_1, \hat{\mathbf{r}}_2) \pm \text{exchange} ] \tag{13}$$

where  $\mathcal{Y}_{l_1 l_2 L}^M(\hat{\mathbf{r}}_1, \hat{\mathbf{r}}_2)$  is a vector-coupled product of spherical harmonics with  $L = 0$  and  $M = 0$ . The generalisation to states of arbitrary  $L$  is straight-forward. The complementary operator  $Q_0$  is then defined by

$$Q^{(0)} = \sum_l \sum_{n_-} |n_-, l\rangle \langle n_-, l| \tag{14}$$

where, for brevity,  $n_-$  stands for all three combinations  $\{+, -\}$ ,  $\{-, +\}$ , and  $\{-, -\}$ , indicating that at least one of the two electrons is in a negative-energy-bound pseudostate.

This method of calculation is similar in spirit to that of Forrey et al. [36] for double-photoionisation of helium, except that the true Coulomb waves are here replaced by pseudostates at the same energy. As shown in Figure 2, the two agree very well out to quite large distances.

The method is justified by the degree to which the final results converge with the basis set size, and the sum over partial waves:

$$\begin{aligned} & \langle \Psi_i(\mathbf{r}_1, \mathbf{r}_2) | P^{(0)} + Q^{(0)} | \Psi_i(\mathbf{r}_1, \mathbf{r}_2) \rangle \\ & = \langle \Psi_i(\mathbf{r}_1, \mathbf{r}_2) | \Psi_i(\mathbf{r}_1, \mathbf{r}_2) \rangle \end{aligned} \tag{15}$$

is satisfied. Instead of analysing the asymptotic form of the scattering solution, as in an  $R$ -matrix calculation, the method analyses the correlated positive energy pseudostate in the region near the nucleus, where the  $Q$  operator projects out that part that has the asymptotic form of a bound state for one of the two electrons. This is then identified as the amplitude for single-ionisation and the orthogonal  $P$  component as the amplitude for double-ionisation. The contrast between the two asymptotic forms is illustrated by comparing the top and bottom panels in Figure 2.

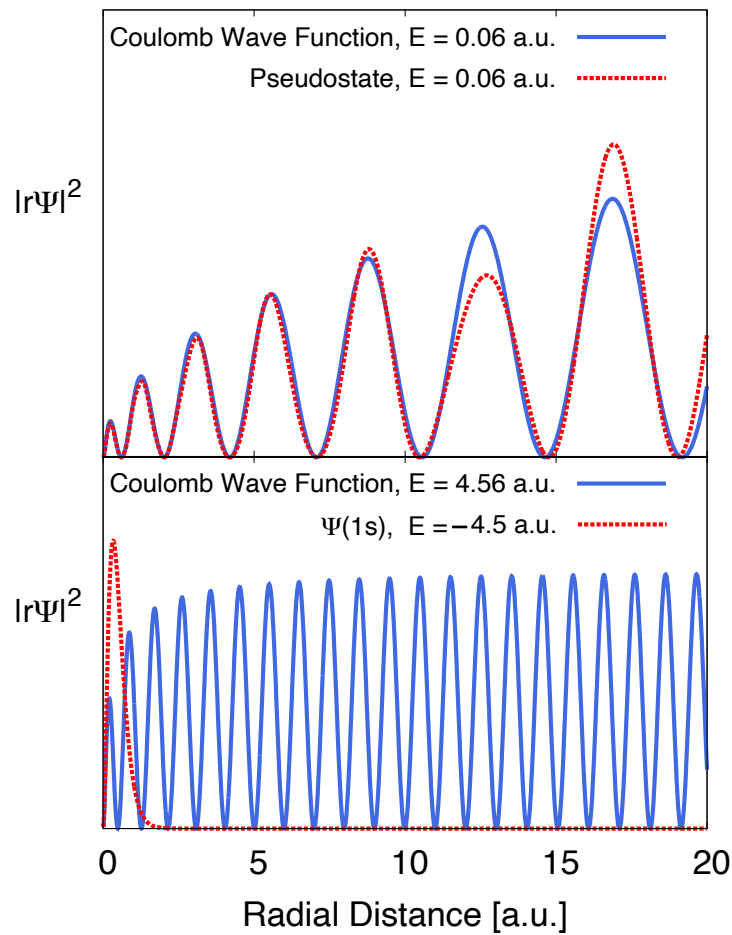


**Figure 2.** Upper panel: Comparison of a one-electron pseudostate radial wave function with the corresponding exact Coulomb wave function at the same energy ( $E = 0.06$  a.u.) near the threshold. For the case of double-ionisation, both electrons have wave functions of this form. This shows that the pseudostate representation remains accurate out to reasonably large distances. Lower panel: The two one-electron states ( $E_{1s} = -4.5$  a.u. and  $E_k = 4.56$  a.u.) corresponding to a near-threshold single-ionisation state, demonstrating that the region nearest the nucleus is that which contributes when taking their product and forming projection operators as described in this paper.

The method must also converge with respect to inclusion of the electron–electron interaction in  $P^{(0)}$  as a perturbation. Up to second order, the perturbed projection operator is

$$P = P^{(0)} + P^{(1)} + P^{(2)} \tag{16}$$

with

$$P^{(1)} = \sum_{n_+} \left[ |n_+\rangle^{(1)} \langle n_+| + |n_+\rangle \langle n_+|^{(1)} \right] \tag{17}$$

and

$$P^{(2)} = \sum_{n_+} \left[ |n_+\rangle^{(2)} \langle n_+| + |n_+\rangle \langle n_+|^{(2)} + |n_+\rangle^{(1)} \langle n_+|^{(1)} \right] \tag{18}$$

where the sum over the zeroth-order two-electron states  $\{n_+\}$  is understood to contain the sum over  $l$  such that the total  $L = 0$  states are formed. The perturbed wave functions are (in the finite set of pseudostates  $|n_+\rangle$ )

$$|n_+\rangle^{(1)} = \sum_{m_+ \neq n_+} |m_+\rangle \alpha_{m_+,n_+} \tag{19}$$

and

$$\alpha_{m,n} = \frac{V_{m,n}}{E_m - E_n} \tag{20}$$

with  $V_{m,n} = \langle m|V|n \rangle$ . The (unnormalised) second-order solutions are

$$\begin{aligned} |n_+\rangle^{(2)} &= \frac{1}{E_{n_+} - H} (V - V_{n_+,n_+}) |n_+\rangle^{(1)} \\ &= |T_{+,+}\rangle + |T_{+,-}\rangle + |T_{-,+}\rangle + |T_{-,-}\rangle \end{aligned} \tag{21}$$

where, for the perturbed state  $|n_+\rangle^{(2)}$ ,

$$|T_{p,q}\rangle = \sum_{\substack{m_p \neq n_+ \\ i_q \neq n_+}} \frac{|m_p\rangle \langle m_p|(V - V_{n_+,n_+})|i_q\rangle}{E_{n_+} - E_{m_p}} \alpha_{i_q,n_+} \tag{22}$$

and  $p$  and  $q$  each take on the values  $+$  or  $-$ . Only  $|T_{+,+}\rangle$  and  $|T_{+,-}\rangle$  contribute to the positive energy projection operator  $P$ , with  $|T_{+,-}\rangle$  corresponding to virtual transitions to negative energy states and back again. The transition probability into the projected final state corresponding to  ${}^6\text{Li}^{3+}$  then corresponds to the diagonal matrix elements:

$$\begin{aligned} |c_i^{3+}|^2 &= \langle \Psi_i({}^6\text{Li}^+) | P^{(0)} + P^{(1)} + P^{(2)} | \Psi_i({}^6\text{Li}^+) \rangle \\ &\equiv |c_i^{(0)3+}|^2 + |c_i^{(1)3+}|^2 + |c_i^{(2)3+}|^2 \end{aligned} \tag{23}$$

The first-order correction  $|c_i^{(1)3+}|^2$  given by

$$|c_i^{(1)3+}|^2 = \sum_{\substack{n_+ \\ m_+ \neq n_+}} \langle \Psi_i | m_+ \rangle \langle n_+ | \Psi_i \rangle \alpha_{m_+,n_+} \tag{24}$$

vanishes identically since the matrix elements are real and  $\alpha_{m_+,n_+} = -\alpha_{n_+,m_+}$ . The second-order correction consists of the diagonal matrix elements of the (0, 2) and the (1, 1) parts, as shown in Equation (18). The (0, 2) part is

$$\begin{aligned} &\sum_{n_+} \left[ |n_+\rangle \langle n_+|^{(2)} + |n_+\rangle^{(2)} \langle n_+| \right] \\ &= \sum_{\substack{n_+ \\ m_+ \neq n_+}} \frac{|n_+\rangle \langle m_+|}{E_{n_+} - E_{m_+}} (V_{m_+,m_+} - V_{n_+,n_+}) \alpha_{m_+,n_+} \\ &+ \sum_{\substack{n_+ \\ m_+ \neq n_+}} \frac{|n_+\rangle \langle m_+|}{E_{n_+} - E_{m_+}} \sum_{i_+ \neq m_+,n_+} V_{m_+,i_+} \alpha_{i_+,n_+} \\ &+ \sum_{\substack{n_+ \\ m_+ \neq n_+}} \frac{|n_+\rangle \langle m_+|}{E_{n_+} - E_{m_+}} \sum_{i_-} V_{m_+,i_-} \alpha_{i_-,n_+} + (n_+ \leftrightarrow m_+) \end{aligned} \tag{25}$$

The first term vanishes because it is antisymmetric under the interchange ( $n_+ \leftrightarrow m_+$ ). The second and third terms can both be rewritten by the use of the identity:

$$\frac{V_{m_+,i_{\pm}} \alpha_{i_{\pm},n_+} - V_{n_+,i_{\pm}} \alpha_{i_{\pm},m_+}}{E_{n_+} - E_{m_+}} = \alpha_{m_+,i_{\pm}} \alpha_{i_{\pm},n_+} \tag{26}$$

to obtain the remaining diagonal part:

$$\begin{aligned} & \sum_{n_+} \left[ |n_+\rangle \langle n_+|^{(2)} + |n_+\rangle^{(2)} \langle n_+| \right] \\ &= \sum_{\substack{n_+ \\ m_+ \neq n_+}} |n_+\rangle \langle m_+| \sum_{i_+ \neq m_+, n_+} \alpha_{m_+, i_+} \alpha_{i_+, n_+} \\ &+ \sum_{\substack{n_+ \\ m_+ \neq n_+}} |n_+\rangle \langle m_+| \sum_{i_-} \alpha_{m_+, i_-} \alpha_{i_-, n_+} \end{aligned} \tag{27}$$

The remaining (1, 1) contribution from Equation (18) is

$$\begin{aligned} & \sum_{n_+} |n_+\rangle^{(1)} \langle n_+|^{(1)} = \sum_{\substack{n_+ \\ m_+ \neq n_+}} |m_+\rangle \langle m_+| \alpha_{m_+, n_+}^2 \\ &+ \sum_{\substack{n_+ \\ m_+ \neq n_+}} \sum_{i_+ \neq m_+, n_+} |m_+\rangle \langle i_+| \alpha_{m_+, n_+} \alpha_{i_+, n_+} \end{aligned} \tag{28}$$

Interchanging the dummy indices  $n_+$  and  $i_+$  shows that the second term cancels the first term of Equation (27), leaving just the terms:

$$\begin{aligned} P^{(2)} &= \sum_{\substack{n_+ \\ m_+ \neq n_+}} |m_+\rangle \langle m_+| \alpha_{m_+, n_+}^2 \\ &+ \sum_{\substack{n_+ \\ m_+ \neq n_+}} |n_+\rangle \langle m_+| \sum_{i_-} \alpha_{m_+, i_-} \alpha_{i_-, n_+} \end{aligned} \tag{29}$$

However, this still must be corrected so that the total wave functions  $|n_+\rangle + |n_+\rangle^{(1)} + |n_+\rangle^{(2)}$  are normalised to unity up to second order. The renormalisation can be accomplished by subtracting a component of the unperturbed solution  $|n_+\rangle$  from  $|n_+\rangle^{(2)}$  to obtain

$$|\tilde{n}_+\rangle^{(2)} = |n_+\rangle^{(2)} - \frac{1}{2} |n_+\rangle \tag{30}$$

which still satisfies the second-order perturbation equation. This contributes an additional amount:

$$\Delta P^{(2)} = - \sum_{n_+, m_+} |m_+\rangle \langle m_+| \alpha_{m_+, n_+}^2 \tag{31}$$

leaving just the renormalised projection operator:

$$\tilde{P}^{(2)} = \sum_{n_+, m_+} |n_+\rangle \langle m_+| \sum_{i_-} \alpha_{m_+, i_-} \alpha_{i_-, n_+} \tag{32}$$

corresponding to the sum over virtual negative energy states.

It turns out that even this contribution is cancelled if one includes the counterbalancing positive energy part coming from the second-order perturbation of negative energy states. Terms from  $|n_-\rangle \langle n_-|^{(2)} + |n_-\rangle^{(2)} \langle n_-|$  do not contribute, but the first-order cross-terms contribute:

$$\sum_{n_-} |n_-\rangle^{(1)} \langle n_-|^{(1)} = \sum_{n_-, m_+ n_+} |m_+\rangle \langle n_+| \alpha_{n_-, m_+} \alpha_{n_-, n_+} \tag{33}$$

With the change of notation  $n_- = i_-$ , it is clear that this term cancels the one remaining term in Equation (32) for  $\tilde{P}^{(2)}$ . Thus, the leading perturbative correction to  $P$  due to the electron–electron interaction is at most of third order. However, it is still of interest to calculate the

$$\sum_i |\tilde{c}_i^{(2)3+}|^2 = \sum_i \langle \Psi_i(^6\text{Li}^+) | \tilde{P}^{(2)} | \Psi_i(^6\text{Li}^+) \rangle \tag{34}$$

contribution (summed over positive energy pseudostates) that would still remain without this final cancellation due to the positive energy part coming from perturbed negative energy states, as discussed in the following section. The second-order contributions from only positive energy states, prior to cancellation, serves as an upper bound on the order at which third- or higher-order effects could contribute.

#### 4. Results and Discussion

This section discusses the numerical results obtained for the transition probability coefficients  $P(^6\text{Li}^{3+}) = \sum_n |c_n^{3+}|^2$  in Equation (23). The calculations are first presented to test for the convergence of the leading coefficients  $\sum_n |c_n^{(0)3+}|^2$  with respect to both  $\Omega_1$  controlling the projection operators and  $\Omega_2$  controlling the pseudospectral Hylleraas representation of the initial and final states. In addition, we examined the convergence with respect to the sum over partial waves  $\ell$  in Equation (12) and perturbation corrections to the projection operators due to the electron–electron Coulomb interaction.

First, concerning the convergence with respect to partial waves, direct calculations were performed up to  $\ell = 7$  (i.e., one-electron states with  $\ell_1 = \ell_2 = \ell$  were coupled to form an  $S$ -state with  $L = 0$ ) and an extrapolation performed up to  $\ell = \infty$ . The results were found to converge relatively slowly in proportion to  $1/\sqrt{\ell + 1}$ . As a typical example, Figure 3 shows the convergence pattern for the  $^6\text{He}(2\ ^3S_1)$  case with  $\Omega_1 = \Omega_2 = 8$ . The extrapolated value is shown by the intercept on the vertical axis.

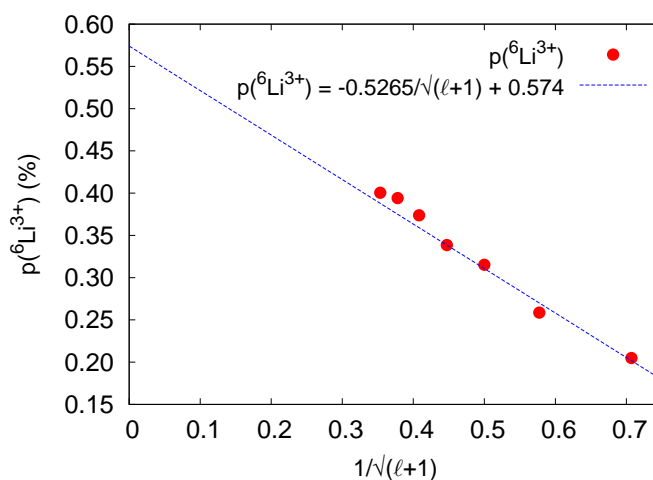


**Figure 3.** An example of convergence, following the beta decay of  $^6\text{He}(1s2s\ ^3S_1)$ , with respect to the number of partial waves  $\ell$  (red dots) for the  $^6\text{Li}^{3+}$  probability for the case  $\Omega_1 = \Omega_2 = 8$ .

Next, concerning the convergence with respect to  $\Omega_1$  and  $\Omega_2$ , the results are shown (as a percentage) by the top number of each pair in Table 2 and for each of the three initial atomic states. The entries along the main diagonal provide a measure of the degree of convergence and their uncertainty. Since there does not appear to be a consistent trend either up or down, we took the average of all the numbers in Table 2 with the rms statistical spread as the uncertainty. The total double-ionisation probability, prior to being subject to the projection operators of Equation (12), is the sum of overlap integrals between an optimised initial state of  $^6\text{He}$  and a pseudospectrum representing all doubly ionised  $^6\text{Li}^+$  states. Although this quantity can be stated with a well-defined error, as demonstrated in [11], it does not show monotonic convergence, but rather, oscillates around a value. The reason for this is that the nonlinear parameters in Equation (6) that are used to variationally diagonalise the Hamiltonian are (necessarily) not separately optimised for each state within the pseudospectrum [37]. The actual numbers of terms in the basis sets for each  $\Omega$  are listed in Table 3.

**Table 2.** Convergence table for the initial states  ${}^6\text{He}(1\ ^1S_0)$ ,  ${}^6\text{He}(2\ ^3S_1)$ , and  ${}^6\text{He}(2\ ^1S_0)$ . All entries are  ${}^6\text{Li}^{3+}$  probabilities (taken in the limit of infinite partial waves, as shown in Figure 3) expressed in % shown for different sizes of both the projection operator ( $\Omega_1$ ) and Hylleraas-type pseudostate ( $\Omega_2$ ) basis sets used in Equation (23). Zeroth- and partial-second-order results from Equation (34) are at the top and bottom of each cell, respectively. The top values in the table for each state will be averaged to obtain the final  ${}^6\text{Li}^{3+}$  probability.

${}^6\text{He State}$	$\Omega_1$	$\Omega_2$			
		8	10	12	14
$1\ ^1S_0$	8	0.3663	0.3564	0.3134	0.4483
		−0.0017	−0.0011	−0.0014	−0.0009
	10	0.3142	0.3326	0.3100	0.4314
		−0.0068	−0.0057	−0.0091	−0.0011
	12	0.3123	0.3145	0.3009	0.4357
		−0.0045	−0.0027	−0.0019	−0.0066
	14	0.3145	0.3128	0.3556	0.4121
		−0.0006	−0.0001	−0.0011	−0.0008
$2\ ^3S_1$	8	0.5740	0.4161	0.4293	0.4028
		−0.0013	−0.0004	−0.0003	−0.0003
	10	0.5084	0.4947	0.5272	0.5405
		−0.0031	−0.0010	−0.0032	−0.0031
	12	0.5223	0.5281	0.5744	0.6209
		−0.0052	−0.0017	−0.0025	−0.0022
	14	0.5304	0.5314	0.6062	0.6400
		−0.0002	−0.0006	−0.0002	−0.0002
$2\ ^1S_0$	8	0.5838	0.4645	0.4829	0.5470
		−0.0041	−0.0036	−0.0027	−0.0030
	10	0.4988	0.5522	0.5611	0.6193
		−0.0284	−0.0083	−0.0196	−0.0467
	12	0.4994	0.5697	0.6046	0.6636
		−0.0023	−0.0089	−0.0012	−0.0052
	14	0.5037	0.5836	0.6196	0.6610
		−0.0027	−0.0001	−0.0034	−0.0010

**Table 3.** Number of terms  $N_1(\Omega_1)$  and  $N_2(\Omega_2)$  in the basis sets. The factor 8 for  $N_1(\Omega_1)$  accounts for the sum over partial waves up to  $\ell = 7$ .

$\Omega_{1\text{or}2}$	$N_1(\Omega_1)$	$N_2(\Omega_2)$		
		$1\ ^1S_0$	$2\ ^3S_1$	$2\ ^1S_0$
8	$81 \times 8$	181	164	182
10	$196 \times 8$	295	218	301
12	$400 \times 8$	442	441	457
14	$729 \times 8$	624	650	652

Finally, concerning perturbation corrections due to the electron–electron interaction, this mixes each of the simple one-electron product pseudostates  $|n_+, \ell\rangle$  with all the others, but as shown in Equation (24), the first-order corrections cancel in pairs when summed over the complete set of states that form the projection operator. A more lengthy calculation in Section 3 shows that the second-order corrections also cancel, provided that one takes into account both the renormalisation of the perturbed wave functions so that  $P^2 = P$  up to second order and the counterbalancing positive energy contribution coming from the perturbed negative energy states. It is perhaps not surprising that these perturbation corrections sum to zero because the only role of the  $P$  projection operator is to enforce

doubly outgoing boundary conditions via positive energy for both electrons without further energy resolution. However, it is still interesting to see the order of magnitude of the partial-second-order contributions generated by  $\tilde{P}^{(2)}$  in Equation (32). The results are shown by the bottom number of each pair in Table 2. Although there is no clear convergence pattern, the magnitudes are all 2% or less of the zero-order term. One can, therefore, expect third- or higher-order contributions not included in the calculation to be smaller still. The main source of uncertainty is thus the convergence uncertainty associated with the zero-order term.

The final results are summarised in Table 4. The main conclusion is that most of the lithium-ions in the energy bin with  $E > 0$  are  ${}^6\text{Li}^{++}$ -ions plus an energetic electron, rather than  ${}^6\text{Li}^{3+}$  plus two low-energy electrons. For example, for the  ${}^6\text{He}(1\ ^1S_0)$  case, of the calculated 1.2(1)% of the  ${}^6\text{Li}$ -ions with  $E > 0$ , 0.35(5)% are  ${}^6\text{Li}^{3+}$ , and the remaining 0.85(10)% are  ${}^6\text{Li}^{++}$ . The  ${}^6\text{Li}^{3+}$  fraction agrees with the 0.32% calculated by Wauters and Vaeck [2], but their total only sums to 99.85%, with no uncertainty given. For the  ${}^6\text{He}(2\ ^1S_0)$  case, the fractions are 0.53(7)% for  ${}^6\text{Li}^{3+}$  and 1.33(7)% for  ${}^6\text{Li}^{++}$ .

The redistributed charge-state fractions are shown in Table 5. However, even these reduced fractions of  ${}^6\text{Li}^{3+}$ -ions are still an order of magnitude or more larger than the experimental values of 0.018(15)% for the  ${}^6\text{He}(1\ ^1S_0)$  case and  $< 0.01\%$  for the  ${}^6\text{He}(2\ ^3S_1)$  case. The recalculated  ${}^6\text{Li}^{++}$  fraction is now also larger than the experiment, while the  ${}^6\text{Li}^+$  fraction remains lower than the experiment. The differences are much larger than the statistical uncertainties. It seems that the theoretical values for both  ${}^6\text{Li}^{++}$  and  ${}^6\text{Li}^{3+}$  need to be lowered by about the same amount and added to  ${}^6\text{Li}^+$  in order to bring the theory and experiments into agreement.

**Table 4.** Previous [11] and corrected  ${}^6\text{Li}^{3+}$  charge-state fractions for each initial state following beta decay. All quantities expressed in percent (%).

${}^6\text{He}$ State	$p({}^6\text{Li}^{3+})$		
	Previous [11]	Present	Exp't
$1\ ^1S_0$	1.2(1)	0.35(5)	0.018(15) [1]
$2\ ^3S_1$	1.86(7)	0.53(7)	$< 0.01$ [9]
$2\ ^1S_0$		0.56(6)	

**Table 5.** Corrected probabilities  $p({}^6\text{Li}^{k+})$  of forming the various charge states of  ${}^6\text{Li}^{k+}$ ,  $k = 1, 2, 3$  following the beta decay of  ${}^6\text{He}(1\ ^1S_0)$  or  ${}^6\text{He}(2\ ^3S_1)$  as initial states. All quantities are expressed in percent (%).

${}^6\text{He}$ State	${}^6\text{Li}$ Ion	Theory		Exp't.	Difference
		Present	Ref. [2]		
$1\ ^1S_0$	${}^6\text{Li}^+$	89.03(3)	89.09	89.9(2) <sup>a</sup>	−0.9(2)
	${}^6\text{Li}^{++}$	10.55(10)	10.44	10.1(2)	0.45(20)
	${}^6\text{Li}^{3+}$	0.35(5)	0.32	0.018(15)	0.34(5)
	Total	99.9(1)	99.85	100.0(2)	−0.1(2)
$2\ ^3S_1$	${}^6\text{Li}^+$	88.711(3)	89.9(3)(1) <sup>b</sup>	−1.2(2)	
	${}^6\text{Li}^{++}$	10.75(7)	10.1(3)(1)	0.65(20)	
	${}^6\text{Li}^{3+}$	0.53(7)	$< 0.01$	0.53(5)	
	Total	99.99(7)	100.00	−0.02(20)	

<sup>a</sup> Carlson et al. [1]. <sup>b</sup> Hong et al. [9].

A possible source of the discrepancy is the failure of the sudden approximation at the  $\pm 1\%$  level of accuracy. A more adiabatic time dependence than a step function would increase the proportion of  ${}^6\text{Li}^+$  at the expense of both  ${}^6\text{Li}^{++}$  and  ${}^6\text{Li}^{3+}$  [38]. For this reason, the results of the sudden approximation represent an upper bound on the amount

of shake-up and shake-off. However, a failure of the sudden approximation at this level would contradict the near-perfect agreement found by Couratin et al. [3] for the case of  ${}^6\text{He}^+$  as the initial state. Their calculation included a perturbation correction to the sudden approximation of only  $-0.02\%$  ( $-0.0002$  relative to unity) to their calculated shake-off fraction of  $2.322\%$ . The sudden approximation as currently implemented also ignored the exchange effects between the beta particle and the atomic electrons [12,13]. However, the effect of the exchange is likely to be small since the beta particle has a much higher energy than the atomic electrons, and a significantly larger effect would again contradict the good agreement for the case of  ${}^6\text{He}^+$ .

In summary, the present work substantially reduced the disagreement between our previous theory [11] and experiments for the  ${}^6\text{Li}^{3+}$  charge-state fraction following the beta decay of both  ${}^6\text{He}(1\ ^1S_0)$  and  ${}^6\text{He}(2\ ^1S_0)$ . It also brought our results into agreement with the CI calculations of Couratin et al. [3] for the  ${}^6\text{He}^+(1s\ ^1S)$  case. However, there remains a substantial disagreement between the theory and experiments for the charge-state fractions, which stands in sharp contrast to the overall excellent agreement found by Couratin et al. for the one-electron case of  ${}^6\text{He}^+$ .

**Author Contributions:** A.T.B. carried out the calculations that were summarised in the Results and Discussion Section. A.T.B. and G.W.F.D. co-developed the underlying theoretical techniques and co-wrote the manuscript. All authors have read and agreed to the published version of the manuscript.

**Funding:** Natural Science and Engineering Research Council of Canada (NSERC) and the Digital Research Alliance of Canada/Compute Ontario.

**Informed Consent Statement:** Not applicable.

**Data Availability Statement:** All data reported in this work are available via direct contact with the corresponding author. The wave functions and matrix element FORTRAN programs used in this work are publicly available at [http://drake.sharcnet.ca/wiki/index.php/Program\\_Notes](http://drake.sharcnet.ca/wiki/index.php/Program_Notes) (accessed on 26 January 2023).

**Acknowledgments:** Research support by the Natural Science and Engineering Research Council of Canada (NSERC), the Digital Research Alliance of Canada/Compute Ontario is gratefully acknowledged. A.T.B. is grateful for the financial support through the NSERC and Queen Elizabeth II scholarships.

**Conflicts of Interest:** The authors declare no conflict of interest.

## References

1. Carlson, T.A.; Pleasonton, F.; Johnson, C.H. Electron Shake Off following the  $\beta^-$  Decay of  ${}^6\text{He}$ . *Phys. Rev.* **1963**, *129*, 2220. [CrossRef]
2. Wauters, L.; Vaeck, N. Study of the electronic rearrangement induced by nuclear transmutations: A B-spline approach applied to the  $\beta$  decay of  ${}^6\text{He}$ . *Phys. Rev. C* **1996**, *53*, 497. [CrossRef] [PubMed]
3. Couratin, C.; Velten, P.; Flechard, X.; Lienard, E.; Ban, G.; Cassimi, A.; Delahaye, P.; Durand, D.; Hennecart, D.; Mauger, F.; et al. First Measurement of Pure Electron Shakeoff in the  $\beta$  Decay of Trapped  ${}^6\text{He}^+$  Ions. *Phys. Rev. Lett.* **2012**, *108*, 243201. [CrossRef] [PubMed]
4. Severijns, N.; Beck, M.; Naviliat-Cuncic, O. Tests of the standard electroweak model in nuclear beta decay. *Rev. Mod. Phys.* **2006**, *78*, 991. [CrossRef]
5. Naviliat-Cuncic, O. Precision correlation measurements in nuclear beta decay. *Phys. Scr.* **2012**, *T150*, 014027. [CrossRef]
6. Gonzalez-Alonso, M.; Naviliat-Cuncic, O.; Severijns, N. New physics searches in nuclear and neutron  $\beta$  decay. *Prog. Particle Nucl. Phys.* **2019**, *104*, 165. [CrossRef]
7. Mukul, I.; Hass, M.; Heber, O.; Hirsh, T.Y.; Rappaport, Y.M.M.L.; Ron, G.; Shachar, Y.; Vaintraub, S. A new scheme to measure the electron-neutrino correlation – the case of  ${}^6\text{He}$ . *arXiv* **2017**, arXiv:1711.08299.
8. Wietfeldt, F.E.; Byrne, J.; Collett, B.; Dewey, M.S.; Jones, G.L.; Komives, A.; Laptev, A.; Nico, J.S.; Noid, G.; Stephenson, E.J.; et al. aCORN: An experiment to measure the electron–antineutrino correlation in neutron decay. *Nucl. Instrum. Methods Phys. Res. A* **2009**, *611*, 207. [CrossRef]
9. Hong, R.; Leredde, A.; Bagdasarova, Y.; Flécharde, X.; García, A.; Knecht, A.; Müller, P.; Naviliat-Cuncic, O.; Pedersen, J.; Smith, E.; et al. Charge-state distribution of Li ions from the  $\beta$  decay of laser-trapped  ${}^6\text{He}$  atoms. *Phys. Rev. A* **2017**, *96*, 053411. [CrossRef]

10. Müller, P.; Bagdasarova, Y.; Hong, R.; Leredde, A.; Bailey, K.G.; Fl'echard, X.; García, A.; Graner, B.; Knecht, A.; Naviliat-Cuncic, O.; et al.  $\beta$ -Nuclear-Recoil Correlation from  ${}^6\text{He}$  Decay in a Laser Trap. *Phys. Rev. Lett.* **2022**, *129*, 182502. [CrossRef]
11. Schulhoff, E.E.; Drake, G.W.F. Electron emission and recoil effects following the beta decay of  ${}^6\text{He}$ . *Phys. Rev. A* **2015**, *92*, 050701. [CrossRef]
12. Cooper, J.W.; Åberg, T. Shaking processes in  $\beta$ -decay. *Nucl. Phys. A* **1978**, *298*, 239. [CrossRef]
13. Saenz, A.; Froelich, P. Effect of final-state interactions in allowed  $\beta$  decays. I. General formalism. *Phys. Rev. C* **1997**, *56*, 2132. [CrossRef]
14. Carter, S.L.; Kelly, H.P. Double photoionization of helium. *Phys. Rev. A* **1981**, *24*, 170. [CrossRef]
15. Sagurton, M.; Bartlett, R.J.; Samson, J.A.R.; He, Z.X.; Morgan, D. Effect of Compton scattering on the double-to-single photoionization ratio in helium. *Phys. Rev. A* **1995**, *52*, 2829. [CrossRef]
16. Bergstrom, P.M.; Hino, K.I.; Macek, J.H. Two-electron ejection from helium by Compton scattering. *Phys. Rev. A* **1995**, *51*, 3044. [CrossRef]
17. Tang, J.-Z.; Shimamura, I. Double photoionization of helium at low photon energies. *Phys. Rev. A* **1995**, *52*, R3413. [CrossRef]
18. Kheifets, A.S.; Bray, I. Calculation of double photoionization of helium using the convergent close-coupling method. *Phys. Rev. A* **1996**, *54*, R995. [CrossRef]
19. Meyer, K.W.; Greene, C.H.; Bray, I. Simplified model of electron scattering using R-matrix methods. *Phys. Rev. A* **1995**, *52*, 1334. [CrossRef]
20. Proulx, D.; Shakeshaft, R. Double ionization of helium by a single photon with energy 89–140 eV. *Phys. Rev. A* **1993**, *48*, R875. [CrossRef]
21. Pont, M.; Shakeshaft, R. Absolute triply differential cross sections for double photoionization of helium at 10, 20, and 52.9 eV above threshold. *Phys. Rev. A* **1995**, *51*, R2676. [CrossRef] [PubMed]
22. Pont, M.; Shakeshaft, R.; Maulbetsch, F.; Briggs, J.S. Angular distributions for double photoionization of helium: Discrepancies between theory and experiment. *Phys. Rev. A* **1996**, *53*, 3671. [CrossRef] [PubMed]
23. Maulbetsch, F.; Briggs, J.S. Angular distribution of electrons following double photoionization. *J. Phys. B At. Mol. Opt. Phys.* **1993**, *26*, 1679. [CrossRef]
24. Sadeghpour, H. Theory of double photoionization in "two-electron" systems. *Can. J. Phys.* **1996**, *74*, 727. [CrossRef]
25. McLaughlin, B.M. An R-matrix with pseudo-state approach to the single photon double ionization and excitation of the He-like  $\text{Li}^+$  ion. *J. Phys. B At. Mol. Opt. Phys.* **2013**, *46*, 075204. [CrossRef]
26. McIntyre, M.W.; Scott, M.P. Photo-double-ionization of He-like and Be-like systems in excited states within an intermediate-energy R-matrix framework. *Phys. Rev. A* **2014**, *89*, 043418. [CrossRef]
27. Kleiman, U.; Pindzola, M.S.; Robicheaux, F. Photoionization with excitation and double photoionization of the  $\text{Li}^+$  ground  $1^1\text{S}$  state and metastable  $2^1,3\text{S}$  states. *Phys. Rev. A* **2005**, *72*, 022707. [CrossRef]
28. Kheifets, A.S.; Bray, I. Photoionization with excitation and double photoionization of the helium isoelectronic sequence. *Phys. Rev. A* **1998**, *58*, 4501. [CrossRef]
29. Hart, H.W.v.; Feng, L. Double photoionization of excited He-like atoms. *J. Phys. B At. Mol. Opt. Phys.* **2001**, *34*, L601. [CrossRef]
30. Drake, G.W.F.; Makowski, A.J. High-precision eigenvalues for the  $1s2p^1P$  and  ${}^3P$  states of helium. *J. Opt. Soc. Am. B* **1988**, *5*, 2207. [CrossRef]
31. Drake, G.W.F.; Yan, Z.-C. Energies and relativistic corrections for the Rydberg states of helium: Variational results and asymptotic analysis. *Phys. Rev. A* **1992**, *46*, 2378. [CrossRef] [PubMed]
32. Drake, G.W.F. *Handbook of Atomic, Molecular, and Optical Physics*; Section 11.3.1; Springer: New York, NY, USA, 2006; pp. 199–219.
33. Berkowitz, J.J. Sum rules and the oscillator strength distribution in helium. *Phys. B At. Mol. Opt. Phys.* **1997**, *30*, 881. [CrossRef]
34. Goldman, S.P.; Drake, G.W.F. Relativistic effects in the photoionization of hydrogenic ions. *Can. J. Phys.* **1983**, *61*, 198. [CrossRef]
35. Drake, G.W.F.; Goldman, S.P. Bethe logarithms for Ps, H, and heliumlike atoms. *Can. J. Phys.* **1999**, *77*, 835. [CrossRef]
36. Forrey, R.C.; Yan, Z.-C.; Sadeghpour, H.R.; Dalgarno, A. Single and double photoionization from dipole response function. *Phys. Rev. Lett.* **1997**, *78*, 3662. [CrossRef]
37. Schulhoff, E.E. Excitation and Ionization of  ${}^6\text{Li}$  Ions following Beta-Decay of  ${}^6\text{He}$ . Master's Thesis, University of Windsor, Windsor, ON, Canada, 2010. Available online: <https://scholar.uwindsor.ca/etd/139/> (accessed on 10 January 2022).
38. Chizma, J.; Karl, G.; Novikov, V.A. Sudden to adiabatic transition in  $\beta$  decay. *Phys. Rev. C* **1998**, *58*, 3674. [CrossRef]

**Disclaimer/Publisher's Note:** The statements, opinions and data contained in all publications are solely those of the individual author(s) and contributor(s) and not of MDPI and/or the editor(s). MDPI and/or the editor(s) disclaim responsibility for any injury to people or property resulting from any ideas, methods, instructions or products referred to in the content.